Communal metabolism by *Methylococcaceae* and *Methylophilaceae* is driving rapid aerobic methane oxidation in sediments of a shallow seep near Elba, Italy

Martin Taubert[1,2,#,*], Carolina Grob[2,#], Andrew Crombie[3], Alexandra M. Howat[2], Oliver J. Burns[3], Miriam Weber[4,5], Christian Lott[4,6], Anne-Kristin Kaster[7,8], John Vollmers[7,8], Nico Jehmlich[9], Martin von Bergen[9,10,11], Yin Chen[12], and J. Colin Murrell[2,*]

[1]Aquatic Geomicrobiology, Institute of Biodiversity, Friedrich Schiller University Jena, Dornburger Str. 159, 07743 Jena, Germany

[2]School of Environmental Sciences, University of East Anglia, Norwich Research Park, Norwich, NR4 7TJ, UK

[3]School of Biological Sciences, University of East Anglia, Norwich Research Park, Norwich, NR4 7TJ, UK

[4]HYDRA Marine Sciences GmbH, Sinzheim, Germany and HYDRA Field Station Elba, Italy

[5]Microsensor Group, Max Plank Institute for Marine Microbiology, Celsiusstr. 1, 28359 Bremen, Germany

[6]Department of Symbiosis, Max Plank Institute for Marine Microbiology, Celsiusstr. 1, 28359 Bremen, Germany

[7]Institute for Biological Interfaces (IBG5), Karlsruhe Institute of Technology, Hermann-von-Helmholtz-Platz 1, 76344 Eggenstein-Leopoldshafen, Karlsruhe, Germany

[8]Leibniz Institute DSMZ - German Collection of Microorganisms and Cell Cultures, Inhoffenstrasse 7B, 38124 Braunschweig, Germany

[9]Department of Molecular Systems Biology, Helmholtz Centre for Environmental Research – UFZ, Leipzig, Germany

[10]Institute of Biochemistry, Faculty of Biosciences, Pharmacy and Psychology, University of Leipzig, Brüderstraße 32, 04103 Leipzig, Germany

[11]Department of Chemistry and Bioscience, University of Aalborg, Fredrik Bajers Vej 7H, 9220 Aalborg East, Denmark.

[12]School of Life Sciences, University of Warwick, Coventry, CV4 7AL, UK.

[#]contributed equally

*Corresponding authors:

Martin Taubert, Aquatic Geomicrobiology, Institute of Biodiversity, Friedrich Schiller University Jena, Dornburger Str. 159, 07743 Jena, Germany; Email: martin.taubert@uni-jena.de; Tel: 00493641 9494 59; Fax:00493641 949462

J. Colin Murrell, School of Environmental Sciences, University of East Anglia, Norwich Research Park, Norwich, NR4 7TJ, UK; Email: j.c.murrell@uea.ac.uk; Tel: 00441603 592959; Fax: 01603 591327

Running title: (50 characters): Aerobic methane oxidation at a shallow seep

The authors declare no conflict of interest.

Originality-Significance Statement

Methane is a potent greenhouse gas contributing substantially to global warming, and emissions from marine seeps contribute up to 10% of methane in the atmosphere. Methanotrophic microorganisms can use methane as carbon and energy source, and thus significantly mitigate global methane emissions from seep areas, acting as an important 'benthic filter'. This study reports on the efficiency and function of the 'benthic filter' at a shallow methane seep, by quantifying the rates of methane oxidation, identifying the microbial key players involved in this process and assessing their function. Compared to the well-studied deep-sea seeps, shallow seeps represent distinct hydrogeochemical settings, where the risk of emitted methane reaching the atmosphere is much higher. The findings we present are highly relevant to evaluate the impact of shallow seeps on global atmospheric methane budgets.

Abstract

Release of abiotic methane from marine seeps into the atmosphere is a major source of this potent greenhouse gas. Methanotrophic microorganisms in methane seeps use methane as carbon and energy source, thus significantly mitigating global methane emissions. Here we investigated microbial methane oxidation at the sediment-water interface of a shallow marine methane seep. Metagenomics and metaproteomics, combined with ^{13}C-methane stable isotope probing, demonstrated that various members of the gammaproteobacterial family *Methylococcaceae* were the key players for methane oxidation, catalyzing the first reaction step to methanol. We observed a transfer of carbon to methanol-oxidizing methylotrophs of the betaproteobacterial family *Methylophilaceae*, suggesting an interaction between methanotrophic and methylotrophic microorganisms that allowed for rapid methane oxidation. From our microcosms, we estimated methane oxidation rates of up to 871 nmol of methane per gram sediment and day. This implies that more than 50% of methane at the seep is removed by microbial oxidation at the sediment-water interface, based on previously reported *in situ* methane fluxes. The organic carbon produced was further assimilated by different heterotrophic microbes, demonstrating that the methane-oxidizing community supported a complex trophic network. Our results provide valuable eco-physiological insights into this specialized microbial community performing an ecosystem function of global relevance.

Introduction

Methane is the most abundant hydrocarbon in the atmosphere, and acts as a harmful greenhouse gas (Reeburgh, 2007). Approximately one third of the global methane flux to the atmosphere is derived from natural sources (Judd et al., 2002b). Reports on the contribution of oceanic methane emissions, primarily originating from natural cold seeps along continental margins (Etiope, 2012), vary from 1 to 10% of the total flux (Kvenvolden et al., 2001; Judd et al., 2002b). The methane flux from the subsurface sea bed, however, is even higher (Reeburgh, 2007). Biological activity of methane-oxidizing microorganisms in seafloor sediments and the water column considerably reduces the amount of methane that reaches the atmosphere. These microorganisms, termed methanotrophs, use methane as their sole carbon and energy source. The methanotrophs act as a 'benthic filter' (Boetius and Wenzhöfer, 2013) modulating methane emission from the sea, and supply methane-derived carbon to a broad range of other organisms. Hence, in the seep environment, methanotrophs carry out a key role in the microbial community that is comparable to autotrophic primary producers, and their activity is affected by the microbial satellite community present (Yu and Chistoserdova, 2017). To understand the modulation of methane emission by the benthic filter, various studies have targeted microbial communities at methane seep areas, especially in the deep sea (see (Boetius and Wenzhöfer, 2013) for a review). Deep-sea sediments are typically characterized by fine-grain particles that limit the circulation of pore water. As the deep-sea seafloor is not influenced by hydrodynamic forces from waves or tidal movement, stable layers with steep hydrogeochemical gradients exist. Oxygen is consumed within the first few millimeters of the sediment through the degradation of organic matter deposited by sedimentation of particulate organic carbon (de Beer et al., 2006; Glud, 2008). Aerobic methane oxidation is hence restricted to a thin layer of sediment, or occurs in microbial mats covering the sediment (Boetius and Wenzhöfer, 2013; Ruff et al., 2016; Paul et al., 2017). In subsurface layers, anaerobic oxidation of methane (AOM) by methanotrophic archaea in combination with sulfate-reducing bacteria takes place, typically

representing the predominant process for methane removal beneath the seafloor (Knittel and Boetius, 2009; Boetius and Wenzhöfer, 2013).

Shallow methane seeps, in contrast, can feature highly permeable sandy sediments, which allow advection-driven pore water circulation that introduces oxygen into deeper layers. The gas flow upwards additionally leads to a downstream of oxic sea water (O'Hara et al., 1995). Further, hydrodynamic forces result in mixing of the sediment and impede the formation of overlying microbial mats. Hence, in contrast to the stable conditions in deep-sea sediments, shallow sediments comprise a highly variable and heterogeneous environment with fluctuating oxygen concentrations. The frequent influx of oxygen restricts the highly oxygen-sensitive AOM consortia to deeper sediment layers (Knittel and Boetius, 2009). Thus, aerobic methane oxidation in the upper layers and at the sediment-water interface might be the predominant process for methane removal at shallow seeps.

Methane originating from depths below 100 m typically does not reach the sea surface due to dissolution processes of methane bubbles and oxidation of dissolved methane (Schmale et al., 2005; McGinnis et al., 2006). Hence, deep-sea seeps play little to no role in atmospheric methane emission. For shallow methane seeps, models suggest site specific parameters such as depth and initial bubble size along with aqueous methane concentration and upwelling flows to be major factors determining methane emission (Leifer and Patro, 2002; McGinnis et al., 2006). Emission from such shallow seeps has been estimated as 310 g CH_4 m^{-2} $year^{-1}$ at the Kattegat coast, Denmark (Dando et al., 1994), up to 550 g CH_4 m^{-2} $year^{-1}$ at Torry Bay, UK (Judd et al., 2002a), 260 g CH_4 m^{-2} $year^{-1}$ at Isla Mocha, Chile (Jessen et al., 2011), and 400 g CH_4 m^{-2} $year^{-1}$ at the Santa Barbara Channel, CA, USA (Luyendyk et al., 2003). The total emissions of the small Kattegat and Torry Bay seeps, covering an area of only a few thousand square meters, are in the range of one metric ton per year, while the Isla Mocha and Santa Barbara Channel seep, covering several square kilometers, are estimated to release 800 to 7200 metric tons of methane per year into the atmosphere.

Little is known about the identity and filter function of aerobic methanotrophic bacteria in such shallow seep areas. In this study, we investigated the diversity and function of aerobic methanotrophs at a shallow methane seep located off the coast of the Island of Elba, Italy, at only 12 meters depth. Discovered in 1995, the Elba shallow methane seep is located in a tectonically-active site (Greve et al., 2014) and is characterized by a gentle, constant bubbling of gas, consisting of up to 73% (Meister et al., 2018) to more than 85% abiotic methane (Ruff et al., 2016; Sciarra et al., 2019), leading to an efflux of 145 g CH_4 m^{-2} $year^{-1}$ into the water column (Sciarra et al., 2019). A previous investigation of AOM at the seep site revealed predominantly sulfur-coupled methane oxidation by consortia resembling those found in deep-sea seeps, but restricted to sediment layers more than 20 cm below the seafloor (Ruff et al., 2016). AOM exhibited only a low methane removal efficiency, and the authors concluded that aerobic methane oxidation is probably more important at this site (Ruff et al., 2016).

Here, we explored the microbial community in the top 2-3 centimeters of the sediment at the Elba methane seep, and its potential for methane oxidation. The aims of our study were (I) to determine the activity of aerobic methanotrophs and estimate their efficiency in methane removal, (II) to identify the key players of methane oxidation active in the oxic sediments, and (III) to follow the flux of methane-derived carbon through the microbial community, assessing the role of methanotrophs as key suppliers of organic carbon at the seep. We combined a ^{13}C-methane stable isotope probing (SIP) approach with metagenomics, to obtain metagenome-assembled genomes (MAGs) of the microorganisms present, as well as metaproteomics, to verify their predicted metabolic functions and assess their activity. This allowed us to gain an understanding of structure and function of the specialized, methanotrophy-driven microbial community at the methane seep.

Results

Activity of methanotrophs in microcosms and estimation of the benthic filter efficiency

A rapid consumption of methane was observed in microcosms containing sediment and water from the Elba shallow methane seep, when supplemented with 1% (v:v, headspace) of ^{12}C- or ^{13}C-methane. Methane consumption started immediately after setup of the microcosms. After 7 days of incubation, methane consumption rates of 439 ± 42 nmol d^{-1} g $sediment^{-1}$ (average of microcosms with ^{12}C and ^{13}C methane, n = 12, ± SD) were observed, with no difference between ^{12}C and ^{13}C incubations (Figure 1). As the high consumption rates led to frequent depletion of methane, we increased the headspace concentration to 2% after 25 days of incubation. This resulted in a significant increase ($p < 0.001$, Student's *t*-test) of methane consumption to 871 ± 123 nmol d^{-1} g $sediment^{-1}$ (average of microcosms with ^{12}C and ^{13}C methane, n = 8, ± SD) (Figure 1). For individual microcosms, methane consumption up to 2.26 µmol d^{-1} g $sediment^{-1}$ was observed (Dataset S1). In comparison, reported methane consumption rates for AOM at the same site were only up to 200 nmol d^{-1} g $sediment^{-1}$ under 1.5 atmospheres of CH_4:CO_2 (90:10) (Ruff et al., 2016).

Using the average rate of methane consumption for 2% headspace concentration, we estimated the annual methane consumption in the Elba methane seep. Based on the sediment porosity given in (Ruff et al., 2016), we calculated a methane consumption of approximately 12 mol m^{-2} $year^{-1}$ (Supplementary Information). Previous studies have reported a gas flow of 0.72 L m^{-2} d^{-1} from the sediment (Sciarra et al., 2019), containing approximately 85% (v:v) methane, resulting in a release of 9 mol m^{-2} $year^{-1}$ methane into the water column. Hence, based on our estimated rates, more than 50% of the methane flowing through the sediment is consumed at the sediment water interface. Indeed, this is likely a considerable underestimation of the *in situ* methane consumption. The methane concentration in the water phase of our microcosms was approximately 22 µM (2% methane), according to calculations based on Henry's Law (Supplementary Information). *In situ*

concentrations at the Elba methane seep are up to one order of magnitude higher, with 50 µM to 550 µM reported for pore water (Ruff et al., 2016). Considering the increase of methane consumption observed in our microcosms when increasing the headspace methane concentration from 1% to 2%, *in situ* consumption could be considerably higher than our estimates. Given that this aerobic removal of methane at the sediment-water-interface exceeds previously reported AOM rates (Ruff et al., 2016), we aimed to explore the function of the underlying microbial methane oxidizing processes.

Identifying the key methane oxidizers

We used an integrated approach combining different 'omics' techniques with SIP to elucidate the key players responsible for the methane consumption observed in our microcosms. Taxonomic profiles of the microbial communities in the microcosms sampled after 25, 45 and 65 days were investigated by metaproteomics to determine the dominant microbial taxa. The majority of peptides identified were consistently related to *Proteobacteria*, with *Alphaproteobacteria* and *Gammaproteobacteria* (including *Betaproteobacteriales*, based on the current Silva taxonomy release 132 (Quast et al., 2013)) being the dominant classes (Figure S1). At the family level, the presence of various taxa implicated in C_1 metabolism was revealed, including *Methylococcaceae* (*Gammaproteobacteria*), *Methylophilaceae* (*Betaproteobacteriales*) and *Rhodobacteraceae* (*Alphaproteobacteria*) (Kalyuzhnaya et al., 2006; Kalyuzhnaya et al., 2012; Ruff et al., 2015). To identify the active methanotrophs, ^{13}C incorporation in peptides extracted from the microcosms amended with ^{13}C-methane was investigated. Peptides related to *Methylococcaceae* as well as *Methylophilaceae* showed ^{13}C relative isotope abundances (RIA) and incorporation patterns suggesting a direct uptake of ^{13}C from methane (Figure 2, Figure S2). Peptides of *Rhodobacteraceae*, however, as well as those of several other taxa, showed incorporation patterns that suggested ^{13}C uptake by cross-feeding rather than by direct uptake of a ^{13}C-labelled substrate. The ^{13}C isotopologue patterns acquired using SIP-metaproteomics allow a differentiation between such modes of carbon assimilation (Seifert et al., 2012; Taubert et al., 2012).

Furthermore, PCR analysis targeting key functional genes for C_1 metabolism was linked with DNA-SIP by investigating the heavy DNA fractions obtained from ^{13}C microcosms. The presence of *pmoA*, encoding the small subunit of the copper-dependent particulate methane monooxygenase (pMMO), as well as of *xoxF*, encoding a lanthanide-dependent methanol dehydrogenase (MDH) (Keltjens et al., 2014; Taubert et al., 2015; Howat et al., 2018) were observed. However, no *mmoX* encoding the alpha-subunit of soluble methane monooxygenase (sMMO), or *mxaF*, encoding a calcium-dependent MDH were found. Interestingly, *pmoA* sequences were exclusively affiliated with *Methylococcaceae*, while *xoxF* sequences were mainly affiliated with *Methylococcaceae*, *Betaproteobacteriales* and *Rhodobacteraceae* (Figure S3). Complementary functional analysis of the metaproteomes likewise revealed that peptides of the pMMO, covering all three subunits PmoCAB, were exclusively affiliated to *Methylococcaceae*. No peptides of other methane oxidizing enzymes, such as sMMO or methyl-coenzyme M reductase (Friedrich, 2005), were found. Peptides of methanol dehydrogenases were exclusively related to XoxF and not to MxaF, and were affiliated to multiple taxonomic groups, including *Methylococcaceae*, *Methylophilaceae* and different *Alphaproteobacteria* (Figure 3). Hence, while multiple taxa were potentially involved in downstream functions like the oxidation of methanol to formaldehyde, only *Methylococcaceae* were able to catalyze the first step in methane degradation, the oxidation of methane to methanol.

To explore the key players for methane oxidation more closely, we conducted SIP-metagenomics by Illumina MiSeq sequencing of the DNA obtained from heavy fractions of the ^{13}C microcosms. Ten million MiSeq reads were assembled and binned, resulting in 99 metagenome-assembled genomes (MAGs), with two MAGs considered complete genome drafts (> 90% completeness, < 5% contamination (Parks et al., 2015; Vollmers et al., 2017a)) and another eight intermediate quality genome drafts (> 70% completeness, < 10% contamination (Bishara et al., 2018) (Figure S4). Surprisingly, eighteen different MAGs affiliated with *Methylococcaceae* were found (Table 1), indicating multiple closely related methane oxidizers. To provide a more accurate taxonomic classification and to estimate relatedness between the different *Methylococcaceae* MAGs, we

performed phylogenetic analysis based on amino acid sequences of single copy marker genes (SCMG) (Wu et al., 2013). All *Methylococcaceae* MAGs contained marker genes that were most closely related to those of *Methylomonas* spp., creating a sister lineage of this genus (Figure 4A). The amino acid identity between the MAGs was typically less than 85%, indicating that indeed multiple closely related species were present.

Genes encoding subunits of pMMO, i.e., *pmoC*, *pmoA* and *pmoB,* were present exclusively in MAGs affiliated with *Methylococcaceae*. The same MAGs typically also contained genes of an ortholog to the *pmoCAB* operon, dubbed *pxmABC* (Figure S5). These orthologs also encode copper-dependent monooxygenases, which are potentially involved in methane oxidation under oxygen limited and nitrite rich conditions (Kits et al., 2015b; Kits et al., 2015a). Potentially linked to these putative alternative pMMOs, several MAGs contained genes involved in denitrification, such as *narG* and *napABC*, encoding nitrate reductases, and *nirS*, encoding nitrite reductase. The expression of the *pmoCAB* genes was confirmed for multiple MAGs (Table 2, Table S1), but no expression of *pxmABC* genes, as well as of the genes involved in denitrification, was observed. No other functional genes for methane-oxidizing enzymes were observed in the metagenomes. Based on both genomic and proteomic data, these bacteria utilized XoxF-type MDHs for oxidation of methanol to formaldehyde. The classification of the MDH genes was verified by phylogenetic analysis using a custom reference database of *xoxF* and *mxaF* genes, clearly placing the detected genes in the *xoxF5* clade (Figure S6). Furthermore, genes of the tetrahydromethanopterin (H_4MPT) pathway for formaldehyde oxidation, as well as key genes of the ribulose monophosphate (RuMP) cycle for formaldehyde assimilation, 3-hexulose-6-phosphate synthase and 3-hexulose-6-phosphate isomerase, were expressed. The identified key players hence showed the typical metabolic traits of type I methanotrophs, in agreement with their taxonomic affiliation within the *Gammaproteobacteria* (Trotsenko and Murrell, 2008).

The gene expression profiles of the different *Methylococcaceae*, as well as the enrichment of their DNA in the heavy fraction and the ^{13}C incorporation in their peptides, demonstrated that several of

these closely related bacteria were active and responsible for methane oxidation in the microcosms. Considering the heterogeneity of the sediment present at the methane seep, these bacteria can have differing environmental preferences, and so their distribution might be driven by hydrogeochemical factors beyond the availability of methane. Hence, despite their taxonomic similarity, these bacteria might inhabit different environmental niches.

Role of non-methanotrophic methylotrophs

In addition to the key methanotrophs, non-methanotrophic organisms affiliated with *Methylophilaceae* were also found to be highly active in the microcosms, as deduced from ^{13}C incorporation. Despite their lack of the ability to oxidize methane, evident from metaproteomic, metagenomic and functional gene data, the ^{13}C incorporation patterns in their peptides were indistinguishable from those of the methanotrophic *Methylococcaceae* (Figure 2, Figure S2), resembling a direct uptake of a ^{13}C labelled substrate (Seifert et al., 2012). Phylogenetic analysis of the six MAGs related to *Methylophilaceae* in our metagenomic dataset, based on amino acid sequences of SCMGs, demonstrated an affiliation with *Methylophilus* spp. and *Methylotenera* spp. (Figure 4B). Functional classification of peptides identified in the metaproteomics analysis showed the presence of XoxF-type methanol dehydrogenases affiliated with the *Methylophilaceae* (clades XoxF4 and XoxF1, Figure S6), as well as enzymes of the H_4MPT pathway for formaldehyde oxidation and the RuMP cycle for formaldehyde assimilation, supporting a methylotrophic lifestyle. The identified peptides could be mapped to several of the six *Methylophilaceae* MAGs observed (Table 2, Table S1), indicating that also from this taxon, different methylotrophs were active in our microcosms.

As no genes or proteins involved in methane oxidation in the *Methylophilaceae* in our microcosms were present, we can exclude that these organisms used methane directly as a carbon source, and instead have more likely been labelled by cross-feeding. For cross-feeding organisms, a shift in the peptide RIA with incubation time can often be detected when newly synthesized, ^{13}C-labelled compounds from the primary consumers mix with pre-existing, unlabelled compounds (Seifert et al.,

2012; Taubert et al., 2012). In our study, we observed such shifts, for instance, in autotrophic *Nitrospirales* (Figure S2) that became labelled due to the enrichment of the carbonate pool in the incubations by $^{13}CO_2$ released from ^{13}C-methane oxidation. However, a low concentration of the respective pre-existing compound, e.g., caused by a starvation period or a rapid uptake by the cross-feeding organisms, will not result in sufficient amounts of intermediately labelled peptides to be detected by metaproteomics analysis. Given the presence of key methylotrophic functions in the *Methylophilaceae*, the most likely explanation for the ^{13}C labelling of these organisms is the uptake of ^{13}C methanol released from the methanotrophic *Methylococcaceae*, implying a transfer of carbon from methanotrophs to methylotrophs.

Interestingly, further putative methylotrophs related to the alphaproteobacterial family *Rhodobacteraceae* were present and active in our microcosms, but showed only indirect ^{13}C incorporation patterns slowly increasing in RIA over time (Figure 2). The low ^{13}C-labelling ratio observed indicated a much slower growth rate than for *Methylophilaceae*. Of 14 MAGs affiliated with *Alphaproteobacteria*, seven were related to the *Roseobacter* clade within the *Rhodobacteraceae*, while the remaining were related to *Hyphomonadaceae*, *Stappiaceae* and an unknown *Rhodobacterales* family (Table 1, Figure S7). Only for one of the MAGs affiliated with the *Roseobacter* clade was a gene encoding a *xoxF*5-type MDH found, as well as the corresponding gene product, indicating that the majority of these bacteria were not able to utilize methanol. Nevertheless, most of the 14 MAGs revealed a metabolic potential for C_1 utilization, typically including glutathione- and tetrahydrofolate-(THF)-dependent pathways for C_1 oxidation/reduction as well as key genes of the serine cycle for formaldehyde assimilation, including hydroxypyruvate reductase, glycerate 2-kinase, malate thiokinase, malyl coenzyme A lyase, isocitrate lyase and crotonyl-CoA reductase. Furthermore, in two of the MAGs affiliated with the *Roseobacter* clade, a gene encoding ribulose bisphosphate carboxylase required for CO_2 fixation was present. The coverage of our metaproteomic analysis was insufficient to verify the metabolism of these alphaproteobacterial organisms. The potential for C_1 utilization suggested that they might assimilate other C_1 compounds potentially

derived from methane oxidation, such as formaldehyde. However, the ^{13}C RIA in the peptides affiliated with *Alphaproteobacteria* was significantly lower than that of *Methylophilaceae* ($p < 0.001$ for all time points, Student's *t*-test), while not significantly different to the autotrophic *Nitrospirales*. This suggested that some of these organisms could have assimilated carbon from CO_2, while using C_1 compounds as energy source (Figure 5). However, the lower RIA observed for *Alphaproteobacteria* might also result from recycling of unlabelled organic compounds in the microcosms. Hence, while our results strongly indicate that the different alphaproteobacterial taxa were continuously active and oxidized C_1 compounds to gain energy in our microcosms, the nature of their carbon source remains uncertain.

Discussion

Previous studies indicated that the activity of methane oxidizing microorganisms leads to a massive reduction of methane emission from marine seeps. Boetius and Wenzhöfer summarized that between 20 and 80% of methane released from cold seeps of continental slopes is removed by this process, depending on the seep environment, with fluid flow rate and oxygen availability as influential parameters (Boetius and Wenzhöfer, 2013). Here we confirmed that this notion holds true for a shallow methane seep near Elba, characterized by highly permeable sandy sediment that allows an increased oxygen circulation into deeper layers. The methane oxidation potential estimated at 12 mol m^{-2} $year^{-1}$, based on rate measurements in microcosms, was in the same range as the methane flux in the water column of 9 mol m^{-2} $year^{-1}$, measured *in situ* (Sciarra et al., 2019), indicating that a major portion of the methane is removed at the sediment-water interface before reaching the water column (Figure 5).

We identified members of the *Methylococcaceae* within the order *Methylococcales* as the key methane oxidizers. Previous studies indicated that *Methylococcales* are typically found at high relative abundance at methane seeps, independent of seep hydrogeochemistry and geographic location (Ruff et al., 2015). Here we showed that the key methane oxidizers present at the Elba seep

formed a sister lineage to *Methylomonas* sp. within the *Methylococcaceae*, potentially comprising a new genus, and that multiple closely related organisms of this taxon were present. This co-occurrence of bacteria from the same functional guild suggests the existence of different niches for methane oxidizers at the sediment-water interface. Parameters like the availability of oxygen and other electron acceptors, the methane concentration and the presence of alternative reduced molecules might drive the distribution of methane oxidizers with different metabolic capabilities. The presence of *pxmABC* genes hints to the potential for nitrite-dependent methanotrophy in the Elba sediments, given suitable conditions (Kits et al., 2015b; Kits et al., 2015a). Furthermore, the substrate-specificity of pMMO-like proteins is often not clear (Tavormina et al., 2013; Khadka et al., 2018), so some *Methylococcaceae* might additionally be capable of oxidizing alternative compounds like short chain alkanes. These divergent metabolic traits would allow the methanotrophs to occupy various niches and thrive under different biogeochemical conditions. Such a functional redundancy provides multiple advantages for ecosystem functions, such as enhanced stability against environmental disturbances (Griffiths and Philippot, 2013). In the shallow, sandy sediment, disturbances can easily occur, e.g., by hydrodynamic forces like waves and currents, or by seasonal changes (Ruff et al., 2016). Moreover, the adaptation of microorganisms to specific environmental niches optimizes their function and hence results in a fine-tuning of the methane oxidation machinery.

Furthermore, the association of methanotrophs with non-methanotrophic methylotrophs seems to be of major importance for the efficiency of methane oxidation. Our results suggested a transfer of methane-derived carbon from the *Methylococcaceae* to methylotrophs related to *Methylotenera* spp. and *Methylophilus* spp. of the *Methylophilaceae*. Interactions of *Methylococcaceae* with other bacteria, e.g., leading to aggregate formation, have been previously reported at deep-sea methane seeps (Ruff et al., 2013). Typically, *Methylophaga* spp. or other gamma- and alphaproteobacterial species are the most abundant methylotrophs associated with the methanotrophic *Methylococcaceae* (Lösekann et al., 2007; Ruff et al., 2013; Ruff et al., 2015; Paul et al., 2017).

352 *Methylophilaceae* related to *Methylotenera*/*Methylophilus* spp., in contrast, are only rarely observed
353 at marine methane seeps (Ruff et al., 2013; Paul et al., 2017). With the notable exception of the
354 OM43 clade (Giovannoni et al., 2008), members of the *Methylophilaceae* family are typically not
355 abundant in marine environments, and seem to prefer environments with lower salinity such as
356 estuaries or freshwater (Kalyuzhnaya et al., 2006; Kalyuzhnaya et al., 2012; Deng et al., 2018).
357 Intriguingly, in sediments of Lake Washington (WA, USA), a well-studied freshwater lake featuring
358 high methane fluxes, cooperations between *Methylococcaceae* and *Methylophilaceae* have been
359 observed as well (Kalyuzhnaya et al., 2008; Beck et al., 2013). Incubation experiments revealed
360 specific relationships between *Methylosarcina* spp. and *Methylophilus* spp. at high oxygen
361 concentrations, as well as *Methylobacter* spp. and *Methylotenera* spp. at lower oxygen
362 concentrations (Hernandez et al., 2015). Synthetic culture experiments with methanotrophic and
363 non-methanotrophic isolates from Lake Washington also revealed *Methylomonas* spp. to be included
364 in such partnerships, and to be highly competitive (Yu et al., 2017). While the non-methanotrophic
365 partners of such interactions obviously benefit from the release of methanol from the
366 methanotrophs, the gain for the methanotrophs is still unclear. An exchange of public goods, such as
367 vitamin B12, or interspecies electron transfer contributing to methane activation have been
368 discussed (Yu and Chistoserdova, 2017). Regardless, the interaction of methanotrophs and
369 methylotrophs is a common theme across various environments featuring high methane fluxes, and
370 seems to be a major factor for efficient functioning of the benthic methane filter (Ho et al., 2014).

371 Methanol and other C_1 compounds are typically produced in marine environments as byproducts of
372 algal growth or decomposition of organic compounds such as osmolytes, resulting in concentrations
373 in the nM to µM range (Naqvi et al., 2005; Beale et al., 2015). Hence, methylotrophs that degrade
374 these compounds are commonly found in marine habitats. These methylotrophs, however, are
375 distinctly different from those present at methane seeps, and are typically dominated by members of
376 the *Roseobacter* clade, the *Methylophilaceae* group OM43 or the SAR11 clade (Giovannoni et al.,
377 2008; Sun et al., 2011; Zhuang et al., 2018). In our microcosms, we found members of the

Roseobacter clade and other *Alphaproteobacteria* with the genetic potential for C_1 utilization. These bacteria showed low, but consistent activity throughout 65 days of incubation. To succeed in the open sea water, these bacteria are optimized for the uptake of the low concentrations of organic compounds present, and usually utilize various C_1 compounds as well as multi-carbon substrates (Brinkhoff et al., 2008), and typically exhibit slow growth rates. In our microcosms, we observed an uptake of methane-derived carbon by these bacteria, but were unable to discern whether they assimilated methanol or other C_1 compounds as byproducts of methane oxidation, or multi-carbon compounds released by the primary C_1 utilizers, or if they fixed CO_2 and used organic carbon compounds solely as energy sources. Such a chemoorganoautotrophic lifestyle, often supported by anoxygenic photosynthesis, has been reported for various marine methylotrophs, termed "methylovores" (Sun et al., 2011; Pinhassi et al., 2016). Hence, although the methane seep recruits a distinct and specific community of C_1-utilizing organisms, apparently the typical marine methylotrophs can also sustain their activity in this environment, and potentially benefit from the increased levels of organic compounds produced by the methanotrophs.

Interestingly, all methanotrophs and methylotrophs of the *Methylococcaceae*, *Methylophilaceae* and other *Alphaproteobacteria* detected in our incubations employed lanthanide-dependent, XoxF-type methanol dehydrogenases instead of the calcium-dependent methanol dehydrogenase MxaFI. The high diversity of *xoxF* gene sequences in marine habitats, especially *xoxF4* and *xoxF5*, as well as their prevalence over *mxaF* gene sequences, has previously been described (Ramachandran and Walsh, 2015; Taubert et al., 2015). The lanthanides required for these enzymes, belonging to the rare earth elements, are typically present in sufficient concentrations in coastal environments from sediments or coastal run-off, despite their low solubility (Elderfield et al., 1990; Keltjens et al., 2014).

In summary, we showed that the microbial community present in the oxic sediments at the Elba methane seep is highly efficient in methane removal, exceeding the methane oxidation rates reported for AOM at this site (Ruff et al., 2016), likely due to the high oxygen levels in the sediment precluding AOM. We identified members of the *Methylococcaceae* as the key players of aerobic

methane oxidation, and obtained several genome drafts of different active, closely related members of this group. We observed a tight association of these methanotrophs with non-methanotrophic methylotrophs of the *Methylophilaceae*, likely through exchange of methanol, contributing to the efficiency of methane oxidation. Finally, methane-derived carbon was also transferred to other microorganisms not able to utilize methanol, supporting the hypothesis that methanotrophs fuel a complex trophic network and can be considered as primary producers in the methane seep environment. The gain of knowledge on methane removal by the 'benthic filter' at shallow seeps provided by our study will facilitate future estimations of the global methane budget, and highlights the relevance of methanotrophs as model systems to study principles of microbial interactions.

Experimental Procedures

Sample collection and microcosm setup

Samples of oxic sediment from the top 2-3 cm and water were collected in May 2014 by divers from a shallow methane seep located off the coast of Elba, Italy (42° 44.628' N, 10° 07.094' E), in 12 m water depth. Five 50 ml BD Falcon™ tubes were filled with ~100 g of sediment each, and two 1 L bottles were filled with seawater from a maximum of 50 cm above the sediment surface. Samples were transported and stored at 4°C until the start of the SIP experiments at the University of East Anglia, United Kingdom, four days after sampling. Microcosms were set up in 120 ml serum bottles with 20 g of sediment and 25 ml of seawater each, and marine ammonium mineral salts (MAMS) were added to a final concentration of 1% of full-strength medium. Microcosms were spiked with 1% (v:v, headspace) ^{13}C-labelled or unlabelled (^{12}C) methane (six of each), and incubated at 25°C in a shaking incubator (50 rpm). Headspace methane concentrations were monitored using gas chromatography (Supplementary Information). When the headspace concentrations in all microcosms were below 0.1% (v:v), additional methane (1-2%, v:v) was added. Duplicate ^{12}C and ^{13}C microcosms were sacrificed for DNA and protein extraction after 25, 45 and 65 days of incubation.

DNA and protein extraction and DNA-SIP

Combined DNA and protein extractions were performed from microcosms as well as from untreated sediment (T0) according to a previously described protocol (Taubert et al., 2012) with minor modifications (Supplementary Information). Extracted DNA was subjected to fractionation using CsCl gradients, and fractions containing ^{13}C-labelled DNA were selected as previously described (Neufeld et al., 2007; Grob et al., 2015) with minor modifications (Supplementary Information).

Amplicon and metagenomic sequencing

PCR amplicons for 454 sequencing were obtained from selected fractions using the following primer sets and conditions: The *pmoA* gene encoding the β-subunit of particulate methane monooxygenase was amplified by nested PCR using primer pairs A189F/A682R (Holmes et al., 1995) and A189F/mb661R (Costello and Lidstrom, 1999) as previously described (Horz et al., 2005). The *mmoX* gene encoding soluble methane monooxygenase subunit A was amplified by nested PCR using primer pairs mmoX166f/mmoX1401r (Auman et al., 2000) and mmoX206f/mmoX886r (Hutchens et al., 2004) as described. The *xoxF4*, *xoxF5* and *mxaF* genes encoding different methanol dehydrogenases were amplified using primer pairs xoxF4f/r, xoxF5f/r (Taubert et al., 2015) and mxaF1003f/mxaF1555r (McDonald and Murrell, 1997) using PCR conditions as described by these authors. Combined and purified triplicate PCR products were subjected to 454 pyrosequencing (GS FLX Titanium system, MR DNA, Shallowater, TX, USA). Sequencing data were processed using mothur (v.1.35.1) (Schloss et al., 2009) for quality control, demultiplexing, and removal of barcodes and primers as previously described for other functional genes (Taubert et al., 2015). Sequences were binned to OTUs with a 97% identity threshold and chimeras were removed using USEARCH (v7.0.1090) (Edgar, 2013). Phylogeny was assigned using Megan (v.5.1.5) (Huson et al., 2011) and a previously described pipeline for functional genes (Dumont et al., 2014). Raw data are available at the National Center for Biotechnology Information (NCBI) database under bioproject PRJNA524087.

For metagenomic sequencing, separate libraries were prepared from total DNA from untreated sediment (T0) as well as from ^{13}C-labelled DNA obtained from the duplicate microcosms of each of the three time points. Metagenomic DNA was sheared using a Covaris S220 sonication device (Covaris Inc., MA, USA) with the following settings: 55 s 175 W, 5% Duty factor, 200 cycles of burst, 55.5 µl. Library preparation was done using the NEBNext® DNA Library Prep kit for Illumina® (E6040, New England BioLabs® Inc., Ipswich, MA, USA). Sufficient material for sequencing (15 - 20 µg) was obtained from SIP fractions without further amplification. Metagenome sequencing was then performed on an Illumina MiSeq machine using v3 chemistry (600 cycles).

Metagenome reads were adapter clipped and quality trimmed using Trimmomatic v0.32 (Bolger et al., 2014). Low complexity reads were removed using the DUST approach of prinseq-lite v0.20.4 (Schmieder and Edwards, 2011) with a cutoff of 15, and residual phiX-contaminants were filtered out using FastQ Screen (Wingett and Andrews, 2018). Overlapping read pairs were then merged using FLASH 1.2.11 (Magoč and Salzberg, 2011).

For each time point and for the untreated samples, an individual metagenome assembly was produced by coassembling the corresponding libraries from experimental replicates using megahit v1.0.5 (Li et al., 2015). Read coverage of assembled contigs was determined by mapping using Bowtie2 (Langmead and Salzberg, 2012). Each metagenome was then binned using Maxbin v.2.1.1 (Wu et al., 2016). Bins were subsequently decontaminated using a z-score based differential coverage approach previously described (Vollmers et al., 2017b; Pratscher et al., 2018). Bins with a high likelihood of originating from the same species were identified based on similarity of coverage profiles across all time points and subsamples, as well as by the presence of nearly identical universal marker genes. Any such related bins were merged and coassembled by extracting the respective reads from all corresponding time points and reassembly using megahit. Completeness and potential contamination of the final binned MAGs was estimated using CheckM (Parks et al., 2015). Phylogenetic trees to elucidate taxonomic relationships for metagenome-assembled genomes based on concatenated amino acid alignments of taxon-specific single copy marker genes were constructed

using the ezTree pipeline (Wu, 2018). The shotgun metagenome reads, corresponding assemblies, as well as binned MAGs with estimated completeness > 70% and contamination < 10% are available at the NCBI database under bioproject PRJNA522277.

SIP-metaproteomics

Sample preparation for metaproteomics analysis was done as previously described (Grob et al., 2015). Mass spectrometry was performed on an Orbitrap Fusion MS (Thermo Fisher Scientific, Waltham, MA, USA) (Supplementary Information).

Proteome Discoverer (v1.4.0288, Thermo Scientific) was used for protein identification and the acquired MS/MS spectra were searched against the NCBI nr database with taxonomy set to Archaea and Bacteria using the Mascot algorithm, and against protein sequences derived from all acquired MAGs using the SequestHT algorithm. Trypsin was chosen as cleavage enzyme, allowing a maximum of two missed cleavages. The precursor mass tolerance (MS) was set to 10 ppm, the fragment mass tolerance (MS/MS) was 0.05 Da. Carbamidomethylation of cysteine was considered as fixed and oxidation of methionine was set as dynamic modification. Peptide spectrum matches (PSMs) were validated using Percolator (v2.04) with a false discover rate (FDR) < 1% and quality filtered for XCorr ≥ 2.25 (for charge state +2) and ≥ 2.5 (for charge state +3). Identified proteins were grouped by applying the strict parsimony principle (Nesvizhskii and Aebersold, 2005). The mass spectrometry proteomics data have been deposited to the ProteomeXchange Consortium via the PRIDE (Perez-Riverol et al., 2019) partner repository with the dataset identifier PXD013378.

Taxonomic classification of peptides was done by the lowest common ancestor method using UniPept (Mesuere et al., 2018). Identification of ^{13}C-labelled peptides and quantification of ^{13}C incorporation was done by comparing measured and expected isotopologue patterns, chromatographic retention times and fragmentation patterns as previously described (Seifert et al., 2012; Taubert et al., 2012). For each taxonomic group of interest, ^{13}C incorporation was quantified in 10 peptides per time point, 5 from each replicate microcosm.

Acknowledgements

The authors are grateful for use of the analytical facilities of the Centre for Chemical Microscopy (ProVIS) at the Helmholtz-Centre for Environmental Research, which is supported by European Regional Development Funds (EFRE – Europe funds Saxony) and the Helmholtz-Association. We thank the HYDRA team for supporting the field sampling campaign. This work was supported by the Gordon and Betty Moore Foundation Marine Microbiology Initiative Grant GBMF3303 to J. Colin Murrell and Yin Chen and through the Earth and Life Systems Alliance, Norwich Research Park, Norwich, UK and by a Leverhulme Trust Early Career Fellowship to Andrew T. Crombie (ECF2016-626).

The authors declare no conflict of interest.

Supplementary information is available at ISME Journal's website.

References

Auman, A.J., Stolyar, S., Costello, A.M., and Lidstrom, M.E. (2000) Molecular characterization of methanotrophic isolates from freshwater lake sediment. *Appl Environ Microb* **66**: 5259-5266.

Beale, R., Dixon, J.L., Smyth, T.J., and Nightingale, P.D. (2015) Annual study of oxygenated volatile organic compounds in UK shelf waters. *Mar Chem* **171**: 96-106.

Beck, D.A.C., Kalyuzhnaya, M.G., Malfatti, S., Tringe, S.G., del Rio, T.G., Ivanova, N. et al. (2013) A metagenomic insight into freshwater methane-utilizing communities and evidence for cooperation between the *Methylococcaceae* and the *Methylophilaceae*. *PeerJ* **1**: e23.

Bishara, A., Moss, E.L., Kolmogorov, M., Parada, A.E., Weng, Z.M., Sidow, A. et al. (2018) High-quality genome sequences of uncultured microbes by assembly of read clouds. *Nat Biotechnol* **36**: 1067-1075.

526 Boetius, A., and Wenzhöfer, F. (2013) Seafloor oxygen consumption fuelled by methane from cold
527 seeps. *Nat Geosci* **6**: 725-734.
528 Bolger, A.M., Lohse, M., and Usadel, B. (2014) Trimmomatic: a flexible trimmer for Illumina sequence
529 data. *Bioinformatics* **30**: 2114-2120.
530 Brinkhoff, T., Giebel, H.A., and Simon, M. (2008) Diversity, ecology, and genomics of the *Roseobacter*
531 clade: a short overview. *Arch Microbiol* **189**: 531-539.
532 Costello, A.M., and Lidstrom, M.E. (1999) Molecular characterization of functional and phylogenetic
533 genes from natural populations of methanotrophs in lake sediments. *Appl Environ Microbiol* **65**:
534 5066-5074.
535 Dando, P.R., Jensen, P., O'Hara, S.C.M., Niven, S.J., Schmaljohann, R., Schuster, U., and Taylor, L.J.
536 (1994) The effects of methane seepage at an intertidal/shallow subtidal site on the shore of the
537 Kattegat, Vendsyssel, Denmark. *B Geol Soc Denmark* **41**: 65-79.
538 de Beer, D., Sauter, E., Niemann, H., Kaul, N., Foucher, J.P., Witte, U. et al. (2006) *In situ* fluxes and
539 zonation of microbial activity in surface sediments of the Håkon Mosby Mud Volcano. *Limnol*
540 *Oceanogr* **51**: 1315-1331.
541 Deng, W.C., Peng, L.L., Jiao, N.Z., and Zhang, Y. (2018) Differential incorporation of one-carbon
542 substrates among microbial populations identified by stable isotope probing from the estuary to
543 South China Sea. *Sci Rep-Uk* **8**: 15378.
544 Dumont, M.G., Lüke, C., Deng, Y.C., and Frenzel, P. (2014) Classification of *pmoA* amplicon
545 pyrosequences using BLAST and the lowest common ancestor method in MEGAN. *Front Microbiol* **5**:
546 34.
547 Edgar, R.C. (2013) UPARSE: highly accurate OTU sequences from microbial amplicon reads. *Nat*
548 *Methods* **10**: 996-998.
549 Elderfield, H., Upstill-Goddard, R., and Sholkovitz, E.R. (1990) The rare earth elements in rivers,
550 estuaries, and coastal seas and their significance to the composition of ocean waters. *Geochim*
551 *Cosmochim Ac* **54**: 971-991.

552 Etiope, G. (2012) Climate science: Methane uncovered. *Nat Geosci* **5**: 373-374.
553 Friedrich, M.W. (2005) Methyl-coenzyme M reductase genes: Unique functional markers for
554 methanogenic and anaerobic methane-oxidizing Archaea. *Method Enzymol* **397**: 428-442.
555 Giovannoni, S.J., Hayakawa, D.H., Tripp, H.J., Stingl, U., Givan, S.A., Cho, J.C. et al. (2008) The small
556 genome of an abundant coastal ocean methylotroph. *Environ Microbiol* **10**: 1771-1782.
557 Glud, R.N. (2008) Oxygen dynamics of marine sediments. *Mar Biol Res* **4**: 243-289.
558 Greve, S., Paulssen, H., Goes, S., and van Bergen, M. (2014) Shear-velocity structure of the Tyrrhenian
559 Sea: Tectonics, volcanism and mantle (de)hydration of a back-arc basin. *Earth Planet Sc Lett* **400**: 45-
560 53.
561 Griffiths, B.S., and Philippot, L. (2013) Insights into the resistance and resilience of the soil microbial
562 community. *FEMS Microbiol Rev* **37**: 112-129.
563 Grob, C., Taubert, M., Howat, A.M., Burns, O.J., Dixon, J.L., Richnow, H.H. et al. (2015) Combining
564 metagenomics with metaproteomics and stable isotope probing reveals metabolic pathways used by
565 a naturally occurring marine methylotroph. *Environ Microbiol* **17**: 4007-4018.
566 Hernandez, M.E., Beck, D.A.C., Lidstrom, M.E., and Chistoserdova, L. (2015) Oxygen availability is a
567 major factor in determining the composition of microbial communities involved in methane
568 oxidation. *PeerJ* **3**: e801.
569 Ho, A., de Roy, K., Thas, O., De Neve, J., Hoefman, S., Vandamme, P. et al. (2014) The more, the
570 merrier: heterotroph richness stimulates methanotrophic activity. *ISME J* **8**: 1945-1948.
571 Holmes, A.J., Costello, A., Lidstrom, M.E., and Murrell, J.C. (1995) Evidence that participate methane
572 monooxygenase and ammonia monooxygenase may be evolutionarily related. *FEMS Microbiol Lett*
573 **132**: 203-208.
574 Horz, H.P., Rich, V., Avrahami, S., and Bohannan, B.J.M. (2005) Methane-oxidizing bacteria in a
575 California upland grassland soil: Diversity and response to simulated global change. *Appl Environ*
576 *Microb* **71**: 2642-2652.

577 Howat, A.M., Vollmers, J., Taubert, M., Grob, C., Dixon, J.L., Todd, J.D. et al. (2018) Comparative
578 genomics and mutational analysis reveals a novel XoxF-utilizing methylotroph in the *Roseobacter*
579 group isolated from the marine environment. *Front Microbiol* **9**: 766.
580 Huson, D.H., Mitra, S., Ruscheweyh, H.J., Weber, N., and Schuster, S.C. (2011) Integrative analysis of
581 environmental sequences using MEGAN4. *Genome Res* **21**: 1552-1560.
582 Hutchens, E., Radajewski, S., Dumont, M.G., McDonald, I.R., and Murrell, J.C. (2004) Analysis of
583 methanotrophic bacteria in Movile Cave by stable isotope probing. *Environ Microbiol* **6**: 111-120.
584 Jessen, G.L., Pantoja, S., Gutiérrez, M.A., Quiñones, R.A., González, R.R., Sellanes, J. et al. (2011)
585 Methane in shallow cold seeps at Mocha Island off central Chile. *Cont Shelf Res* **31**: 574-581.
586 Judd, A.G., Sim, R., Kingston, P., and McNally, J. (2002a) Gas seepage on an intertidal site: Torry Bay,
587 Firth of Forth, Scotland. *Cont Shelf Res* **22**: 2317-2331.
588 Judd, A.G., Hovland, M., Dimitrov, L.I., García-Gil, S., and Jukes, V. (2002b) The geological methane
589 budget at continental margins and its influence on climate change. *Geofluids* **2**: 109-126.
590 Kalyuzhnaya, M.G., Bowerman, S., Lara, J.C., Lidstrom, M.E., and Chistoserdova, L. (2006)
591 *Methylotenera mobilis* gen. nov., sp nov., an obligately methylamine-utilizing bacterium within the
592 family *Methylophilaceae*. *Int J Syst Evol Micr* **56**: 2819-2823.
593 Kalyuzhnaya, M.G., Beck, D.A.C., Vorobev, A., Smalley, N., Kunkel, D.D., Lidstrom, M.E., and
594 Chistoserdova, L. (2012) Novel methylotrophic isolates from lake sediment, description of
595 *Methylotenera versatilis* sp nov and emended description of the genus *Methylotenera*. *Int J Syst Evol*
596 *Micr* **62**: 106-111.
597 Kalyuzhnaya, M.G., Lapidus, A., Ivanova, N., Copeland, A.C., McHardy, A.C., Szeto, E. et al. (2008)
598 High-resolution metagenomics targets specific functional types in complex microbial communities.
599 *Nat Biotechnol* **26**: 1029-1034.
600 Keltjens, J.T., Pol, A., Reimann, J., and Op den Camp, H.J.M. (2014) PQQ-dependent methanol
601 dehydrogenases: rare-earth elements make a difference. *Appl Microbiol Biot* **98**: 6163-6183.

602 Khadka, R., Clothier, L., Wang, L., Lim, C.K., Klotz, M.G., and Dunfield, P.F. (2018) Evolutionary history
603 of copper membrane monooxygenases. *Front Microbiol* **9**.
604 Kits, K.D., Klotz, M.G., and Stein, L.Y. (2015a) Methane oxidation coupled to nitrate reduction under
605 hypoxia by the Gammaproteobacterium *Methylomonas denitrificans*, sp nov type strain FJG1. *Environ*
606 *Microbiol* **17**: 3219-3232.
607 Kits, K.D., Campbell, D.J., Rosana, A.R., and Stein, L.Y. (2015b) Diverse electron sources support
608 denitrification under hypoxia in the obligate methanotroph *Methylomicrobium album* strain BG8.
609 *Front Microbiol* **6**.
610 Knittel, K., and Boetius, A. (2009) Anaerobic oxidation of methane: Progress with an unknown
611 process. *Annu Rev Microbiol* **63**: 311-334.
612 Kvenvolden, K.A., Lorenson, T.D., and Reeburgh, W.S. (2001) Attention turns to naturally occurring
613 methane seepage. *EOS, Transactions American Geophysical Union* **82**: 457-457.
614 Langmead, B., and Salzberg, S.L. (2012) Fast gapped-read alignment with Bowtie 2. *Nat Methods* **9**:
615 357-359.
616 Leifer, I., and Patro, R.K. (2002) The bubble mechanism for methane transport from the shallow sea
617 bed to the surface: A review and sensitivity study. *Cont Shelf Res* **22**: 2409-2428.
618 Li, D., Liu, C.M., Luo, R., Sadakane, K., and Lam, T.W. (2015) MEGAHIT: an ultra-fast single-node
619 solution for large and complex metagenomics assembly via succinct *de Bruijn* graph. *Bioinformatics*
620 **31**: 1674-1676.
621 Lösekann, T., Knittel, K., Nadalig, T., Fuchs, B., Niemann, H., Boetius, A., and Amann, R. (2007)
622 Diversity and abundance of aerobic and anaerobic methane oxidizers at the Haakon Mosby mud
623 volcano, Barents Sea. *Appl Environ Microb* **73**: 3348-3362.
624 Luyendyk, B., Washburn, L., Banerjee, S., Clark, J., and Quigley, D. (2003) A methodology for
625 investigation of natural hydrocarbon gas seepage in the northern Santa Barbara channel. *OCS Study*
626 *MMS 2003* **54**: 1-66.

627 Magoč, T., and Salzberg, S.L. (2011) FLASH: fast length adjustment of short reads to improve genome
628 assemblies. *Bioinformatics* **27**: 2957-2963.
629 McDonald, I.R., and Murrell, J.C. (1997) The methanol dehydrogenase structural gene *mxaF* and its
630 use as a functional gene probe for methanotrophs and methylotrophs. *Appl Environ Microb* **63**: 3218-
631 3224.
632 McGinnis, D.F., Greinert, J., Artemov, Y., Beaubien, S.E., and Wüest, A. (2006) Fate of rising methane
633 bubbles in stratified waters: How much methane reaches the atmosphere? *J Geophys Res-Oceans*
634 **111**.
635 Meister, P., Wiedling, J., Lott, C., Bach, W., Kuhfuss, H., Wegener, G. et al. (2018) Anaerobic methane
636 oxidation inducing carbonate precipitation at abiogenic methane seeps in the Tuscan archipelago
637 (Italy). *PLoS One* **13**.
638 Mesuere, B., Van der Jeugt, F., Willems, T., Naessens, T., Devreese, B., Martens, L., and Dawyndt, P.
639 (2018) High-throughput metaproteomics data analysis with Unipept: A tutorial. *J Proteomics* **171**: 11-
640 22.
641 Naqvi, S.W.A., Bange, H.W., Gibb, S.W., Goyet, C., Hatton, A.D., and Upstill-Goddard, R.C. (2005)
642 Biogeochemical ocean-atmosphere transfers in the Arabian Sea. *Prog Oceanogr* **65**: 116-144.
643 Nesvizhskii, A.I., and Aebersold, R. (2005) Interpretation of shotgun proteomic data - The protein
644 inference problem. *Mol Cell Proteomics* **4**: 1419-1440.
645 Neufeld, J.D., Vohra, J., Dumont, M.G., Lueders, T., Manefield, M., Friedrich, M.W., and Murrell, J.C.
646 (2007) DNA stable-isotope probing. *Nat Protoc* **2**: 860-866.
647 O'Hara, S.C.M., Dando, P.R., Schuster, U., Bennis, A., Boyle, J.D., Chui, F.T.W. et al. (1995) Gas seep
648 induced interstitial water circulation - observations and environmental implications. *Cont Shelf Res*
649 **15**: 931-948.
650 Parks, D.H., Imelfort, M., Skennerton, C.T., Hugenholtz, P., and Tyson, G.W. (2015) CheckM: assessing
651 the quality of microbial genomes recovered from isolates, single cells, and metagenomes. *Genome*
652 *Res* **25**: 1043-1055.

Paul, B.G., Ding, H.B., Bagby, S.C., Kellermann, M.Y., Redmond, M.C., Andersen, G.L., and Valentine, D.L. (2017) Methane-oxidizing bacteria shunt carbon to microbial mats at a marine hydrocarbon seep. *Front Microbiol* **8**: 186.

Perez-Riverol, Y., Csordas, A., Bai, J., Bernal-Llinares, M., Hewapathirana, S., Kundu, D.J. et al. (2019) The PRIDE database and related tools and resources in 2019: improving support for quantification data. *Nucleic Acids Res* **47**: D442-D450.

Pinhassi, J., DeLong, E.F., Béjà, O., González, J.M., and Pedrós-Alió, C. (2016) Marine bacterial and archaeal ion-pumping rhodopsins: genetic diversity, physiology, and ecology. *Microbiol Mol Biol R* **80**: 929-954.

Pratscher, J., Vollmers, J., Wiegand, S., Dumont, M.G., and Kaster, A.K. (2018) Unravelling the identity, metabolic potential and global biogeography of the atmospheric methane-oxidizing upland soil cluster alpha. *Environ Microbiol* **20**: 1016-1029.

Quast, C., Pruesse, E., Yilmaz, P., Gerken, J., Schweer, T., Yarza, P. et al. (2013) The SILVA ribosomal RNA gene database project: improved data processing and web-based tools. *Nucleic Acids Res* **41**: D590-D596.

Ramachandran, A., and Walsh, D.A. (2015) Investigation of XoxF methanol dehydrogenases reveals new methylotrophic bacteria in pelagic marine and freshwater ecosystems. *FEMS Microbiol Ecol* **91**.

Reeburgh, W.S. (2007) Oceanic methane biogeochemistry. *Chem Rev* **107**: 486-513.

Ruff, S.E., Biddle, J.F., Teske, A.P., Knittel, K., Boetius, A., and Ramette, A. (2015) Global dispersion and local diversification of the methane seep microbiome. *P Natl Acad Sci USA* **112**: 4015-4020.

Ruff, S.E., Arnds, J., Knittel, K., Amann, R., Wegener, G., Ramette, A., and Boetius, A. (2013) Microbial communities of deep-sea methane seeps at Hikurangi continental margin (New Zealand). *PLoS One* **8**: e72627.

Ruff, S.E., Kuhfuss, H., Wegener, G., Lott, C., Ramette, A., Wiedling, J. et al. (2016) Methane seep in shallow-water permeable sediment harbors high diversity of anaerobic methanotrophic communities, Elba, Italy. *Front Microbiol* **7**: 374.

679 Schloss, P.D., Westcott, S.L., Ryabin, T., Hall, J.R., Hartmann, M., Hollister, E.B. et al. (2009)
680 Introducing mothur: open-source, platform-independent, community-supported software for
681 describing and comparing microbial communities. *Appl Environ Microbiol* **75**: 7537-7541.
682 Schmale, O., Greinert, J., and Rehder, G. (2005) Methane emission from high-intensity marine gas
683 seeps in the Black Sea into the atmosphere. *Geophys Res Lett* **32**.
684 Schmieder, R., and Edwards, R. (2011) Quality control and preprocessing of metagenomic datasets.
685 *Bioinformatics* **27**: 863-864.
686 Sciarra, A., Saroni, A., Etiope, G., Coltorti, M., Mazzarini, F., Lott, C. et al. (2019) Shallow submarine
687 seep of abiotic methane from serpentinized peridotite off the Island of Elba, Italy. *Appl Geochem*
688 **100**: 1-7.
689 Seifert, J., Taubert, M., Jehmlich, N., Schmidt, F., Volker, U., Vogt, C. et al. (2012) Protein-based stable
690 isotope probing (protein-SIP) in functional metaproteomics. *Mass Spectrom Rev* **31**: 683-697.
691 Sun, J., Steindler, L., Thrash, J.C., Halsey, K.H., Smith, D.P., Carter, A.E. et al. (2011) One carbon
692 metabolism in SAR11 pelagic marine bacteria. *PLoS One* **6**: e23973.
693 Taubert, M., Grob, C., Howat, A.M., Burns, O.J., Dixon, J.L., Chen, Y., and Murrell, J.C. (2015) *XoxF*
694 encoding an alternative methanol dehydrogenase is widespread in coastal marine environments.
695 *Environ Microbiol* **17**: 3937-3948.
696 Taubert, M., Vogt, C., Wubet, T., Kleinsteuber, S., Tarkka, M.T., Harms, H. et al. (2012) Protein-SIP
697 enables time-resolved analysis of the carbon flux in a sulfate-reducing, benzene-degrading microbial
698 consortium. *ISME J* **6**: 2291-2301.
699 Tavormina, P.L., Ussler, W., Steele, J.A., Connon, S.A., Klotz, M.G., and Orphan, V.J. (2013) Abundance
700 and distribution of diverse membrane-bound monooxygenase (Cu-MMO) genes within the Costa Rica
701 oxygen minimum zone. *Env Microbiol Rep* **5**: 414-423.
702 Trotsenko, Y.A., and Murrell, J.C. (2008) Metabolic aspects of aerobic obligate methanotrophy. *Adv*
703 *Appl Microbiol* **63**: 183-229.

Vollmers, J., Wiegand, S., and Kaster, A.K. (2017a) Comparing and evaluating metagenome assembly tools from a microbiologist's perspective - Not only size matters! *PLoS One* **12**: e0169662.

Vollmers, J., Frentrup, M., Rast, P., Jogler, C., and Kaster, A.K. (2017b) Untangling genomes of novel planctomycetal and verrucomicrobial species from Monterey Bay kelp forest metagenomes by refined binning. *Front Microbiol* **8**: 472.

Wingett, S.W., and Andrews, S. (2018) FastQ Screen: A tool for multi-genome mapping and quality control. *F1000Research* **7**: 1338.

Wu, D.Y., Jospin, G., and Eisen, J.A. (2013) Systematic identification of gene families for use as "markers" for phylogenetic and phylogeny-driven ecological studies of bacteria and archaea and their major subgroups. *PLoS One* **8**: e77033.

Wu, Y.W. (2018) ezTree: an automated pipeline for identifying phylogenetic marker genes and inferring evolutionary relationships among uncultivated prokaryotic draft genomes. *BMC Genomics* **19**: 921.

Wu, Y.W., Simmons, B.A., and Singer, S.W. (2016) MaxBin 2.0: an automated binning algorithm to recover genomes from multiple metagenomic datasets. *Bioinformatics* **32**: 605-607.

Yu, Z., and Chistoserdova, L. (2017) Communal metabolism of methane and the rare earth element switch. *J Bacteriol* **199**.

Yu, Z., Beck, D.A.C., and Chistoserdova, L. (2017) Natural selection in synthetic communities highlights the roles of *Methylococcaceae* and *Methylophilaceae* and suggests differential roles for alternative methanol dehydrogenases in methane consumption. *Front Microbiol* **8**: 2392.

Zhuang, G.C., Peña-Montenegro, T.D., Montgomery, A., Hunter, K.S., and Joye, S.B. (2018) Microbial metabolism of methanol and methylamine in the Gulf of Mexico: insight into marine carbon and nitrogen cycling. *Environ Microbiol* **20**: 4543-4554.

Figure and Table Legends

Figure 1: Methane consumption in microcosms with sediment from the Elba methane seep. Values given are the cumulative amount of methane consumed in the microcosms. Separate averaged values for microcosms with ^{12}C-methane and microcosms with ^{13}C-methane are depicted by cross and diamond symbols , respectively. Error bars indicate standard deviation. Arrows indicate time points of methane addition. Brackets display the amount of methane (% headspace, v:v) of each 737 addition and number of replicate microcosms (n) each supplemented with ^{12}C- or ^{13}C- methane.

Figure 2: ^{13}C incorporation into peptides of different bacterial taxonomic groups. Values depict (A) the ^{13}C relative isotope abundance (RIA), i.e., the amount of carbon replaced by ^{13}C, and (B) the labelling ratio, i.e., the abundance of ^{13}C-labelled compared to unlabelled molecules, of peptides specific to the given taxonomic groups after incubation of sediment for 25, 45 and 65 days with ^{13}C-methane. Values are based on n = 10 peptides per time point, error bars show standard deviation.

Figure 3: Functional classification of identified peptides. The numbers of peptides affiliated to different enzymes and pathways of different functional categories relevant for C_1 metabolism are shown. Colors depict the taxonomic distribution of the peptides in each functional category based on the lowest common ancestor of each peptide. Peptide identification is based on metaproteomics analysis of samples from microcosms with ^{12}C-methane of all three time points (n = 6). The peptides were identified using NCBI nr and the metagenome-assembled genomes obtained in this study as reference databases. MMO: methane monooxygenase, MDH: methanol dehydrogenase, FAE: formaldehyde-activating enzyme, H4MPT: tetrahydromethanopterin pathway for formaldehyde oxidation, THF: tetrahydrofolate pathway for formaldehyde oxidation, glutathione: glutathione pathway for formaldehyde oxidation, formate DH: formate dehydrogenase, RuMP: ribulose monophosphate pathway, based on the key enzymes 3-hexulose-6-phosphate synthase and 3-hexulose-6-phosphate isomerase. For the serine cycle, the key enzymes hydroxypyruvate reductase,

glycerate 2-kinase, malate thiokinase, malyl coenzyme A lyase, isocitrate lyase and crotonyl-CoA reductase were taken into account. For the Calvin cycle, the key enzyme ribulose-1,5-bisphosphate carboxylase/oxygenase was taken into account.

Figure 4: Phylogenetic affiliation of the key methanotrophs and methylotrophs identified at the Elba methane seep. (A) Phylogenetic tree representing key methanotrophs, based on a concatenated amino acid alignment of 36 single copy marker genes with a total of 6 329 positions. Only metagenome-assembled genomes (MAGs) related to *Methylococcaceae* with at least 50% completeness are shown. *Pseudomonas oryzae* (*Pseudomonadales*) was included as an outgroup to root the tree. (B) Phylogenetic tree representing key methylotrophs, based on a concatenated amino acid alignment of 94 single copy marker genes with a total of 21 475 positions. Only MAGs related to *Methylophilaceae* with at least 35% completeness are shown. *Sulfuricella denitrificans* (*Gallionellaceae*) was included as an outgroup to root the tree. Both trees were inferred with the Approximately-Maximum-Likelihood approach of FastTree using the JTT-CAT model for amino acid evolution, local support values were calculated using the Shimodaira-Hasegawa test from 1 000 resamples. The scale bars indicate the number of amino acid changes per site.

Figure 5: Conceptual overview of communal methane metabolism at the Elba seep. The character C in red indicates methane-derived carbon. OC: organic carbon compounds released from the primary methane utilizing community of *Methylococcaceae* and *Methylophilaceae*. *Methane consumption of the microbial community estimated based on average consumption rates in microcosms from this study. $^{+}$Methane flux from sediments to hydrosphere as reported in Ruff et al., 2015 (Ruff et al., 2015).

Table 1: Statistics for metagenome-assembled genomes affiliated with *Methylococcaceae*, *Methylophilaceae* and other *Alphaproteobacteria*. Taxonomic relationships were elucidated based on concatenated amino acid alignments of taxon-specific single copy marker genes using the ezTree

779 pipeline (Wu, 2018). [1]Based on CheckM analysis (Parks et al., 2015). N50: 50% of the genome
780 assembly is contained in scaffolds equal to or larger than this value.

781 **Table 2: Presence and expression of functional genes for C_1 metabolism in metagenome-assembled**
782 **genomes.** White fields indicate presence of functional genes for the respective function, red fields
783 indicate expression of the encoded enzymes based on metaproteomics analysis. Numbers in the
784 fields indicate number of genes expressed / number of genes present. [1]Based on key genes 3-
785 hexulose-6-phosphate synthase and 3-hexulose-6-phosphate isomerase. [2]Based on key genes
786 hydroxypyruvate reductase, glycerate 2-kinase, malate thiokinase, malyl coenzyme A lyase, isocitrate
787 lyase and crotonyl-CoA reductase. [3]Based on key gene ribulose-1,5-bisphosphate
788 carboxylase/oxygenase.

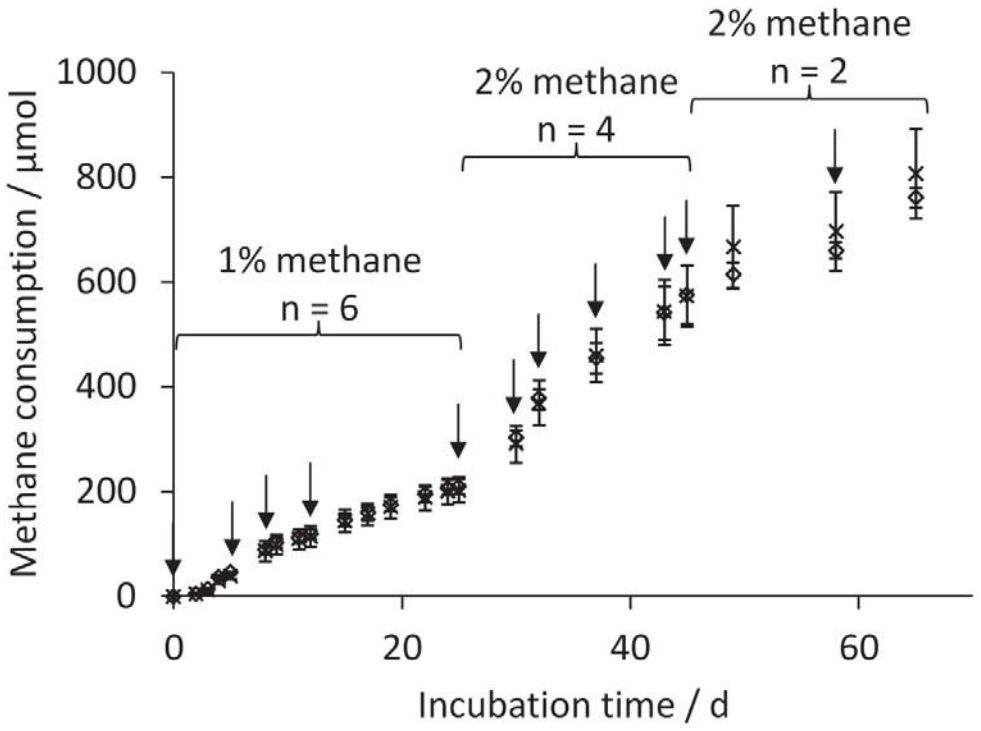

Figure 1: Methane consumption in microcosms with sediment from the Elba methane seep. Values given are the cumulative amount of methane consumed in the microcosms. Separate averaged values for microcosms with ^{12}C-methane and microcosms with ^{13}C-methane are depicted by cross and diamond symbols, respectively. Error bars indicate standard deviation. Arrows indicate time points of methane addition. Brackets display the amount of methane (% headspace, v:v) of each addition and number of replicate microcosms (n) each supplemented with ^{12}C- or ^{13}C-methane.

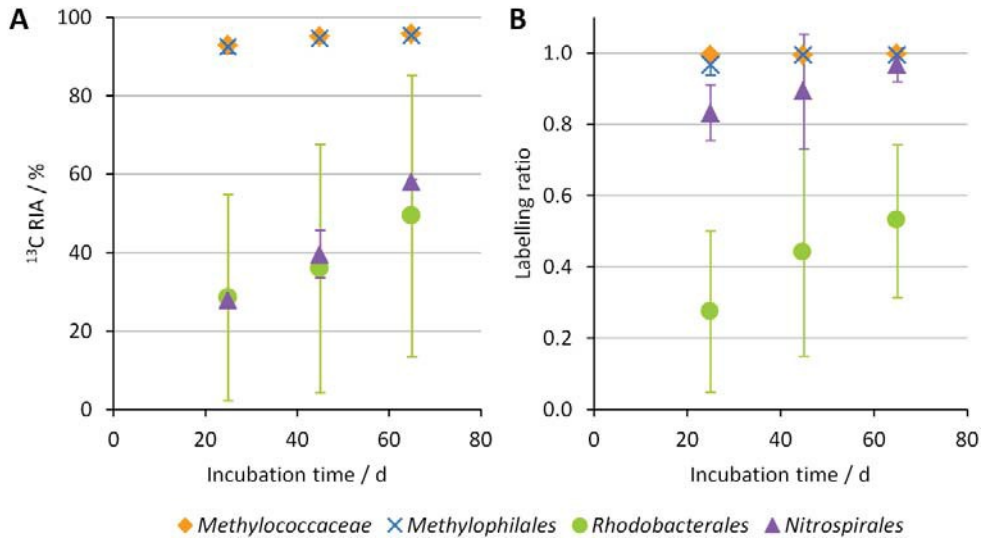

Figure 2: ^{13}C incorporation into peptides of different bacterial taxonomic groups. Values depict (A) the ^{13}C relative isotope abundance (RIA), i.e., the amount of carbon replaced by ^{13}C, and (B) the labelling ratio, i.e., the abundance of ^{13}C-labelled compared to unlabelled molecules, of peptides specific to the given taxonomic groups after incubation of sediment for 25, 45 and 65 days with ^{13}C-methane. Values are based on n = 10 peptides per time point, error bars show standard deviation.

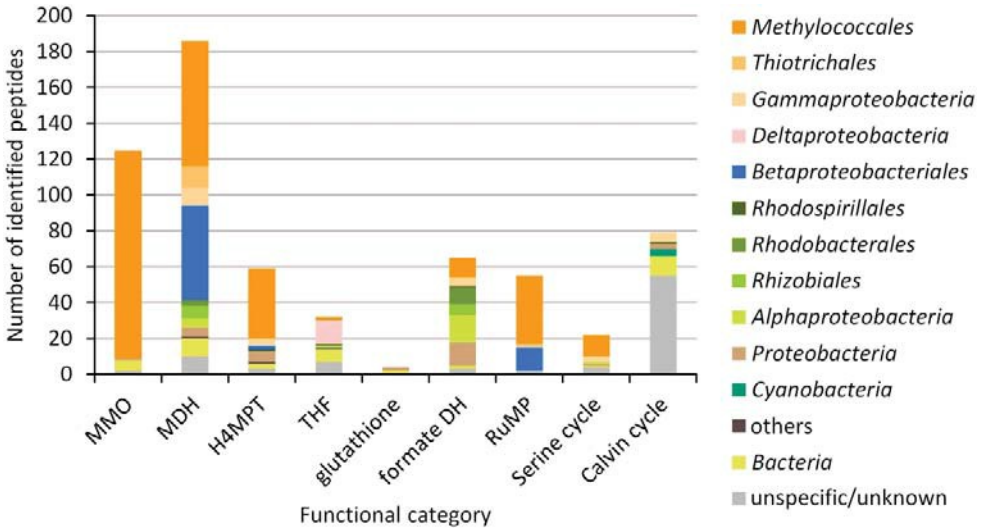

Figure 3: Functional classification of identified peptides. The numbers of peptides affiliated to different enzymes and pathways of different functional categories relevant for C_1 metabolism are shown. Colors depict the taxonomic distribution of the peptides in each functional category based on the lowest common ancestor of each peptide. Peptide identification is based on metaproteomics analysis of samples from microcosms with ^{12}C-methane of all three time points (n = 6). The peptides were identified using NCBI nr and the metagenome-assembled genomes obtained in this study as reference databases. MMO: methane monooxygenase, MDH: methanol dehydrogenase, FAE: formaldehyde-activating enzyme, H4MPT: tetrahydromethanopterin pathway for formaldehyde oxidation, THF: tetrahydrofolate pathway for formaldehyde oxidation, glutathione: glutathione pathway for formaldehyde oxidation, formate DH: formate dehydrogenase, RuMP: ribulose monophosphate pathway, based on the key enzymes 3-hexulose-6-phosphate synthase and 3-hexulose-6-phosphate isomerase. For the serine cycle, the key enzymes hydroxypyruvate reductase, glycerate 2-kinase, malate thiokinase, malyl coenzyme A lyase, isocitrate lyase and crotonyl-CoA reductase were taken into account. For the Calvin cycle, the key enzyme ribulose-1,5-bisphosphate carboxylase/oxygenase was taken into account.

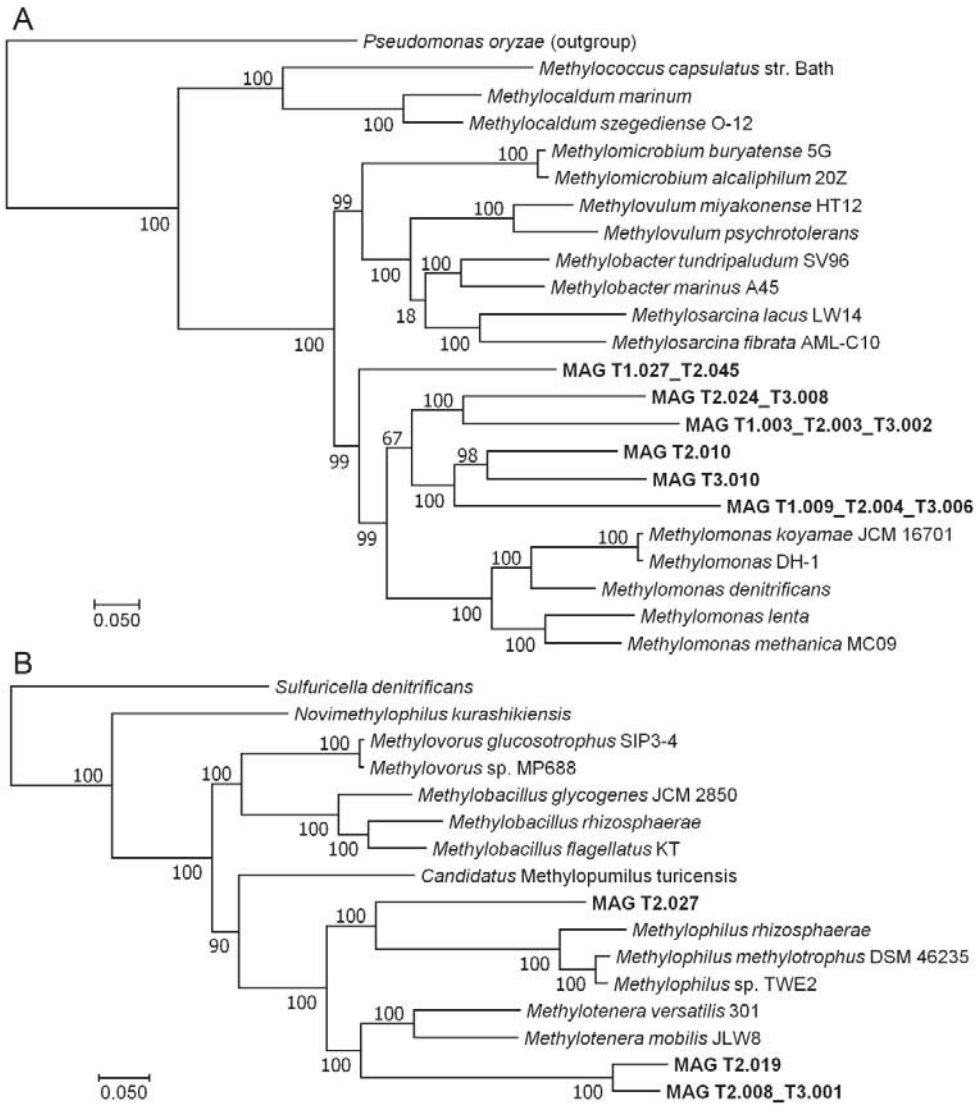

Figure 4: Phylogenetic affiliation of the key methanotrophs and methylotrophs identified at the Elba methane seep. (A) Phylogenetic tree representing key methanotrophs, based on a concatenated amino acid alignment of 36 single copy marker genes with a total of 6 329 positions. Only metagenome-assembled genomes (MAGs) related to *Methylococcaceae* with at least 50% completeness are shown. *Pseudomonas oryzae* (*Pseudomonadales*) was included as an outgroup to root the tree. (B) Phylogenetic tree representing key methylotrophs, based on a concatenated amino acid alignment of 94 single copy marker genes with a total of 21 475 positions. Only MAGs related to *Methylophilaceae* with at least 35% completeness are shown. *Sulfuricella denitrificans* (*Gallionellaceae*) was included as an outgroup to root the tree. Both trees were inferred with the Approximately-Maximum-Likelihood approach of FastTree using the JTT-CAT model for amino acid evolution, local support values were calculated using the Shimodaira-Hasegawa test from 1 000 resamples. The scale bars indicate the number of amino acid changes per site.

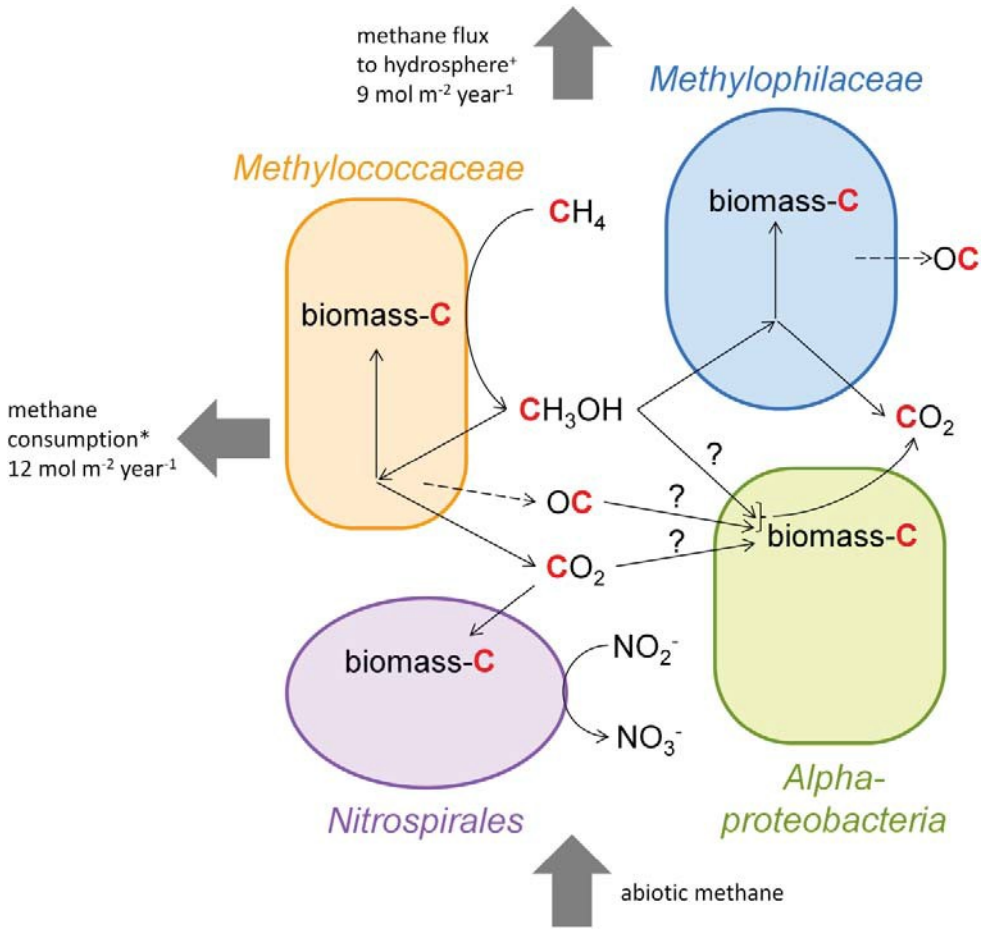

Figure 5: Conceptual overview of communal methane metabolism at the Elba seep. The character C in red indicates methane-derived carbon. OC: organic carbon compounds released from the primary methane utilizing community of *Methylococcaceae* and *Methylophilaceae*. *Methane consumption of the microbial community estimated based on average consumption rates in microcosms from this study. +Methane flux from sediments to hydrosphere as reported in Ruff et al., 2015 (Ruff et al., 2015).

Table 1

MAG ID	Completeness [1] / %	Contamination [1] / %	Genome size / bp	# scaffolds	N50 / bp	Longest scaffold / bp	GC-content / %	Taxonomy
T2.024_T3.008	100	1.7	3683201	376	34899	93907	44.2	*Methylococcaceae*
T1.009_T2.004_T3.006	83	0.0	2300148	655	4880	22077	41	
T1.003_T2.003_T3.002	83	1.7	3077222	293	75471	205488	45.4	
T2.010	79	12.9	2913017	643	6449	30650	43.2	
T3.010	70	1.7	1589959	663	2776	11559	39.9	
T1.027_T2.045	54	0.0	2190210	498	6013	23572	50.7	
T1.007_T2.016_T3.009	48	21.9	2527797	1237	2234	22330	46.4	
T1.019_T2.038	44	10.0	890090	349	3371	21537	41	
T1.030	32	0.0	555941	75	11159	37635	43.5	
T1.008	28	0.0	1494445	617	3100	17312	40	
T2.043	22	0.0	362264	189	2000	6705	43.8	
T3.014	19	0.0	758301	465	1669	5485	42.2	
T2.026	18	0.0	717869	348	2219	9852	42.4	
T1.022	17	1.9	412297	304	1307	3810	40.5	
T2.011	17	3.5	444422	193	2739	15981	45	
T1.002	13	1.7	389904	210	1836	8026	45.4	
T2.056	12	0.0	433371	233	1946	5949	41.5	
T1.005	12	1.7	357089	217	1700	5296	42.9	
T2.027	90	7.6	1688246	192	19805	82017	43.8	*Methylophilaceae*
T2.008_T3.001	84	8.6	2242488	316	40778	107604	44.5	
T2.019	36	0.0	1151259	154	18334	44712	45.4	
T2.058	20	0.0	313978	123	2860	10416	44.3	
T2.018	16	0.0	672373	229	3746	22975	44.5	
T2.053	8	2.7	237367	104	2715	8566	44.5	
T2.009	91	0.0	2013842	46	107948	212351	54.8	*Rhodobacterales*
T2.007	88	0.0	2945199	280	15984	62688	57.7	*Rhodobacterales*
T2.006_T3.003	71	1.7	3450492	222	63712	159910	56.7	*Rhodobacterales*
T2.015	57	0.3	2302051	202	19356	68546	59.1	*Hyphomonadaceae*
T2.014	47	1.7	1805201	302	10348	38924	58.2	*Rhodobacterales*
T2.023	45	7.5	1925340	1179	1653	8054	54.3	*Alphaproteobacteria*
T2.054	42	0.0	1519802	590	3097	12667	50.4	*Alphaproteobacteria*
T3.011	36	0.0	1629932	595	3299	11661	57.4	*Hyphomonadaceae*
T1.014	35	0.0	826762	285	3403	12803	49.6	*Rhodobacterales*
T2.029	25	1.0	1825719	1003	1936	7230	56.9	*Labrenzia*
T1.018	18	3.8	803406	573	1353	4436	57.9	*Hyphomonadaceae*
T1.016	17	0.0	1413249	817	1778	10583	57.9	*Rhodobacterales*
T2.033	13	3.5	251432	198	1245	2899	58.2	*Alphaproteobacteria*
T1.015_T2.022	4	0.0	593602	408	1414	5020	64.1	*Rhodobacterales*

Table 2

		methane oxidation			methanol oxidation		C_1 oxidation				C_1 assimilation		
	MAG ID	methane monooxygenase/ammonia monooxygenase (*pmo*)	soluble methane monooxygenase (*mmo*)	methyl-coenzyme m reductase (*mcr*)	methanol dehydrogenase (*mxaF*)	methanol dehydrogenase (*xoxF*)	tetrahydromethanopterine (H4MPT) pathway for formaldehyde oxidation	tetrahydrofolate (THF) pathway for formaldehyde oxidation	glutathione pathway for formaldehyde oxidation	formate dehydrogenase	ribulose monophosphate pathway [1]	serine pathway [2]	Calvin-Benson-Bassham cycle [3]
Methylococcaceae	T2.024_T3.008	3 / 3				1 / 1	3 / 14	0 / 3			3 / 3	0 / 4	
	T1.009_T2.004_T3.006	2 / 5				1 / 1	3 / 14	0 / 2		0 / 2	2 / 4	0 / 4	
	T1.003_T2.003_T3.002	1 / 8				1 / 1	1 / 9	0 / 3	0 / 1	1 / 1	1 / 2	0 / 4	
	T2.010	0 / 6					1 / 21	0 / 4	0 / 2	0 / 1	1 / 1	0 / 7	
	T3.010						2 / 9	0 / 1		0 / 1		0 / 3	
	T1.027_T2.045	0 / 2				1 / 1	1 / 8	0 / 3		0 / 1	2 / 2	0 / 1	
	T1.007_T2.016_T3.009	0 / 7					1/ 23	0 / 9	0 / 1	0 / 3		0 / 1	
	T1.019_T2.038					2 / 2	0 / 9			0 / 1		0 / 2	
	T1.030											0 / 3	
	T1.008	1 / 1				1 / 1	0 / 1	0 / 1				0 / 3	
	T2.043						0 / 2						
	T3.014	2 / 4					0 / 4	0 / 1				0 / 3	
	T2.026						1 / 5	0 / 2				0 / 2	
	T1.022	0 / 1					0 / 2	0 / 1		0 / 1		0 / 4	
	T2.011	0 / 9					0 / 5	0 / 1		0 / 1			
	T1.002	3 / 4					0 / 3						
	T2.056						0 / 2	0 / 1					
	T1.005	1 / 3						0 / 1					
Methylophilaceae	T2.027					1 / 1	1 / 9	0 / 3		0 / 1	0 / 3		
	T2.008_T3.001					2 / 4	0 / 7	0 / 3		0 / 1	2 / 3		
	T2.019					0 / 1	0 / 7	0 / 2		0 / 2	0 / 1		
	T2.058							0 / 1					
	T2.018						0 / 3	0 / 3		0 / 1			
	T2.053					2 / 2	1 / 4			0 / 1	0 / 1		
Alphaproteobacteria	T2.009							0 / 2	0 / 1			0 / 3	
	T2.007							0 / 3	0 / 2	1 / 2		0 / 7	0 / 1
	T2.006_T3.003							0 / 3	1 / 3			0 / 12	0 / 1
	T2.015							0 / 2	0 / 2			1 / 5	
	T2.014							0 / 2	0 / 2	0 / 1		0 / 3	
	T2.023							0 / 2	0 / 2	1 / 3		0 / 3	
	T2.054							0 / 2	0 / 2	0 / 1		0 / 1	
	T3.011							0 / 1	0 / 3			0 / 4	
	T1.014							0 / 1				0 / 1	
	T2.029							0 / 2	0 / 2	2 / 2		0 / 2	
	T1.018							0 / 1	0 / 3			0 / 5	
	T1.016							0 / 2				0 / 3	
	T2.033											0 / 1	
	T1.015_T2.022					1 / 1	1 / 1	1 / 3				0 / 2	